

be obtained by using πr_0^2 for $\bar{\sigma}_p$ and $(2m\epsilon_p)^{1/2}$ for p , with m near to the true mass of a He³ atom. Then Eq. (2) becomes

$$\Gamma_p \approx (\epsilon_p E_F)^{1/2}. \quad (3)$$

Consequently, for large p , there is no cutoff, and the quasiparticles are like real particles and are relatively well defined in the sense that $\Gamma_p \ll \epsilon_p$.

The region in which Γ_p is comparable to ϵ_p and the quasiparticles are not well defined depends upon the way in which Γ_p varies between the two limits given by Eqs. (1) and (3), and this requires a more detailed calculation. A smooth interpolation suggests that Γ_p/ϵ_p may not be greater than 1 and so, for example, the cut-off factor $(2/\pi) \tan^{-1}(\epsilon_p/\Gamma_p)$ used by Morel and Nozières⁵ may not be less than 0.5. Although this would have some consequences for the effective interaction, presumably they would be less drastic than those found by Cohen and Abrahams,¹ particularly since intermediate states of quite high momentum are important for scattering in relative D states.

These considerations do not allow a firm conclusion about the effects of quasiparticle lifetimes but they do indicate the necessity of a more detailed calculation.

Finally, in the high-momentum approximation which has been used, the mean free path is about 3 Å which is of the same order as the range of the van der Waals force so that collisions of three or more particles are important

in determining Γ_p for $\epsilon_p \geq E_F$. The elementary theory of dense gases⁸ indicates that these effects would increase Γ_p by about 50%. The same problem also arises in the calculation of Λ since, in Eq. (1), Γ_p should be regarded as the lifetime of a quasiparticle rather than a real particle. This may be a significant source of the disagreement⁹ between the independent-pair approximations and experiment.

This Letter had its origin in a conversation with Dr. J. Weneser and I have profited from discussion with him and with Dr. S. Kahana and Professor R. E. Peierls.

[†]Work performed under the auspices of the U. S. Atomic Energy Commission.

¹R. W. Cohen and E. Abrahams, Phys. Rev. Letters **16**, 931 (1966).

²K. E. Brueckner, T. Soda, P. W. Anderson, and P. Morel, Phys. Rev. **118**, 1442 (1960).

³V. J. Emery and A. M. Sessler, Phys. Rev. **119**, 43 (1960).

⁴J. Bardeen, L. N. Cooper, and J. R. Schrieffer, Phys. Rev. **108**, 1175 (1957).

⁵P. Morel and P. Nozières, Phys. Rev. **126**, 1909 (1962).

⁶Equation (1) was obtained in this way by Morel and Nozières.

⁷I. Ulehla, L. Gomolcak, and Z. Pluhar, Optical Model of the Atomic Nucleus (Publishing House of the Czechoslovak Academy of Sciences, Prague, 1964).

⁸S. Chapman and T. G. Cowling, The Mathematical Theory of Nonuniform Gases (Cambridge University Press, Cambridge, 1952), 2nd ed.

⁹V. J. Emery, Ann. Phys. (N.Y.) **28**, 1 (1964).

RELAXATION TIME, EFFECTIVE MASS, AND STRUCTURE OF IONS IN LIQUID HELIUM*

Arnold J. Dahm[†]

School of Physics, University of Minnesota, Minneapolis, Minnesota

and

T. M. Sanders, Jr.

H. M. Randall Laboratory, University of Michigan, Ann Arbor, Michigan

(Received 15 June 1966)

We have measured the momentum relaxation time of ions in liquid helium II by a microwave technique. This new information, in combination with existing data on ion mobilities, makes it possible for the first time to evaluate the effective masses of the carriers.¹

The effective mass of the positive ion is determined to be tens of helium masses and to be temperature-dependent, and its known properties can be given a consistent interpretation

in terms of the electrostriction model² and simple hydrodynamic reasoning. For the negative carrier, our data indicate an effective mass larger than that of the positive ion, and thus clearly rule out any model of the nearly-free-electron type.³ The results are not inconsistent with the bubble model.⁴

Our experiment involved a measurement of the microwave conductivity due to a collection of ions introduced into a reflection cavity, res-

onant at approximately 9.3 GHz. Similar techniques have previously been applied to the study of carriers in gases⁵ and solids.⁶ The experiment is most simply analyzed in terms of a time-averaged Langevin equation (sometimes referred to⁷ as "the equation of motion for the drift velocity"). The equation is

$$\vec{F} = e\vec{\mathcal{E}} = M^* \left(\frac{d\vec{v}}{dt} + \frac{\vec{v}}{\tau} \right). \quad (1)$$

Here τ and M^* are a phenomenological relaxation time and an effective mass, respectively. For the case of a dc field, this equation leads to the familiar result

$$\vec{v} = \mu(0)\vec{\mathcal{E}} = (e\tau/M^*)\vec{\mathcal{E}}. \quad (2)$$

When the field varies in time as $e^{i\omega t}$, the drift velocity becomes

$$\vec{v} = \mu(\omega)\vec{\mathcal{E}} = \left\{ \mu(0)\vec{\mathcal{E}} / [1 + (\omega\tau)^2] \right\} (1 - i\omega\tau), \quad (3)$$

where $\mu(\omega)$ is the mobility at frequency ω .

When a sample of carriers is introduced into a microwave cavity, the (complex) reflection coefficient, Γ , of the cavity will change by an amount proportional to the (complex) mobility. A measurement of the ratio of the imaginary part of Γ , Γ_i , to the real part, Γ_r , yields $\omega\tau$ directly. The effective mass can then be obtained from the measured dc mobility by use of Eq. (2). Alternatively, if Γ_i cannot be measured, $\omega\tau$ can be obtained from a measurement of Γ_r alone, if all parameters determining the absorption (Γ_r) signal are known except the factor $[1 + (\omega\tau)^2]$ in (3). We have been forced to use this second, and less reliable, method because of a very high level of noise and pick-up when our apparatus was made sensitive to dispersion (Γ_i).

The reflection cavity is contained in one arm of a two-bolometer bridge (homodyne) spectrometer, permitting measurement of the complex reflection coefficient.⁸ The cylindrical cavity, which is used in the TE_{011} mode, is shown in Fig. 1. A 50-mCi Po^{210} α emitter produces ionization in the extension tube, which is fabricated of copper rings, insulated from each other, and is beyond cutoff for 3-cm microwaves. A dc field in the source region determines which polarity ion is studied. A 1-kV peak-to-peak square wave, applied between successive rings in the extension tube, chops the ion beam. The carriers are then drawn through the cavity by dc potentials applied to the rings making up the walls of the cavity. The iris plate, at the

top of the cavity, is insulated from the cavity walls and the coupling wave guide, and is used as a current collector. The output of the bolometer detectors is fed to a narrow-band amplifier and phase-sensitive detector, whose reference signal is derived from the same source as the beam-chopping square wave. In this way the spectrometer is made sensitive to changes in the cavity reflection coefficient arising from introduction of the ions.

The change in the real part of the reflection coefficient due to the ions, which is the quantity that we measure, can be written in the form⁹

$$\delta\Gamma_r = \left\{ \frac{2\pi Q_0 e\mu(0)}{\omega[1 + (\omega\tau)^2]} \right\} \cdot \frac{\int n(\vec{r})\vec{\mathcal{E}}_m^2(\vec{r})d^3r}{\int \vec{\mathcal{E}}_m^2(\vec{r})d^3r}. \quad (4)$$

Here Q_0 is the unloaded Q of the cavity, and $n(\vec{r})$ and $\mathcal{E}_m(\vec{r})$ are, respectively, the density of ions and the microwave electric field at a position \vec{r} in the cavity. To calculate $\omega\tau$, we had to determine the density distribution of the ions in the cavity. The fact that the iris current was measured greatly simplified this problem. The dc field distribution in the cavity was studied in an electrolytic tank, and from this measurement the charge distribution (including space-charge effects) was calculated. The Q of the cavity was measured during each

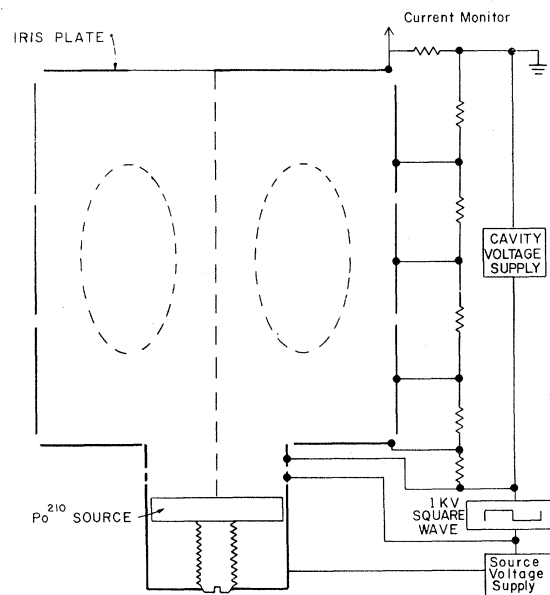


FIG. 1. Cross section of microwave cavity. The square of the microwave electric field inside the dashed ellipse is larger than half-maximum.

run. All other factors relating $\delta\Gamma_\gamma$ to the deflection of the output recorder of the spectrometer were also determined, and were checked to fair accuracy by use of the cavity and spectrometer in an electron spin-resonance measurement. Thus the only unknown quantity in Eq. (4) is $\omega\tau$, which can then be determined.

In Fig. 2 we plot the quantity

$$m^* \equiv \frac{e}{\omega\mu(0)} \cdot \left(\frac{\mu(0)}{\mu_r(\omega)} - 1 \right)^{1/2} = e(\omega\tau)/\omega\mu(0) = M^* \quad (5)$$

as a function of temperature for positive ions.¹⁰ The error bars include allowances for all sources of error except in the values of $\mu(0)$ and the sensitivity of the spectrometer, which we believe to have been constant, but uncertain by $\pm 15\%$. An error in this quantity would shift all the points, but would not greatly alter the shape of the curve.

Figure 2 also shows the experimental data for the negative carrier. No useful points were obtained above 2°K , where the mobility is low, or below 1.7°K , where the negative current drops to very low values.¹¹

The positive-ion data can apparently be understood in terms of the electrostriction model. In this model the Coulomb field around a point charge causes a pressure (and density) gradient in the vicinity of the charge. At some distance R from the ion, the pressure equals the melting pressure, $P_m(T)$. Inside R the helium is solid. R can be calculated using the known elastic properties of liquid helium. An approximate expression, sufficiently accurate for the present discussion, is

$$R = \left\{ [(\epsilon - 1)e^2] / [8\pi\epsilon^2(P_m - P_0)] \right\}^{1/4}. \quad (6)$$

Here ϵ is the dielectric constant of liquid helium, and P_0 , the ambient pressure.

At low temperatures, where $\rho_n \ll \rho_s \approx \rho$, we may calculate the effective mass of such a sphere using inviscid hydrodynamics. The usual result,¹²

$$M^* = M + \frac{1}{2}\rho_s \times \frac{4}{3}\pi R^3 \quad (T \ll T_\lambda) \quad (7)$$

predicts

$$M^* = (47 + 13)M_{\text{He}}.$$

Here M is the mass of the solid sphere of radius R . At temperatures near T_λ , on the other hand, where the mean free path of the elementary excitations is small compared to R ,

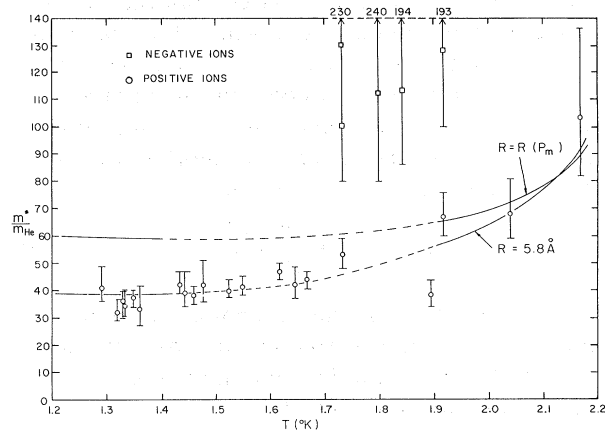


FIG. 2. The experimental quantity, m^* , in units of the helium atomic mass versus temperature for positive and negative ions. Expression (7) is shown by the solid lines in the low-temperature region for $R = 5.8 \text{ \AA}$ and for $R = R(P_m)$ evaluated from (6). Expression (11) with M^* evaluated from (8) is shown by the solid lines at higher temperatures for the same radii. A dashed line connects the contribution of the viscosity to the effective mass is uncertain. The numbers at the top of the graph are the upper limits of the experimental errors for the negative ions.

we can also calculate a contribution to the effective mass of a sphere oscillating at frequency ω from viscous flow in the normal fluid.¹³ Adding together the contributions from the normal and superfluid components, we obtain the expression

$$M^* = M + \frac{1}{2}\rho \times \frac{4}{3}\pi R^3 \left[1 + \frac{2}{3}(\rho_n \delta / \rho R) \right] \quad (T < T_\lambda) \quad (8)$$

with

$$\delta \equiv [2\eta / \omega\rho_n]^{1/2}.$$

Here η is the normal fluid viscosity, and δ is the penetration depth.

In this temperature region we cannot analyze the motion of the ions in terms of Eq. (1), but must consider the viscous drag of the normal fluid on the ions. The equation for the drift velocity is¹³

$$M^*(d\vec{v}/dt) + 6\pi\eta R(1 + R/\delta)\vec{v} = e\vec{\mathcal{E}}. \quad (9)$$

Solving for the real part of the microwave mobility we obtain

$$\mu_r(\omega) = \frac{\mu(0)}{(1 + R/\delta)} \left\{ 1 + \left[\frac{\omega\mu(0)M^*}{e(1 + R/\delta)} \right]^2 \right\}^{-1}. \quad (10)$$

The relationship between the effective mass, M^* , and the experimental quantity, m^* , plotted in Fig. 2 is

$$m^* \equiv \frac{e}{\omega \mu(0)} \left[\frac{\mu(0)}{\mu_r(\omega)} - 1 \right]^{1/2} \\ = \left[\left(\frac{e}{\omega \mu(0)} \right)^2 \frac{R}{\delta} + \frac{(M^*)^2}{(1+R/\delta)} \right]^{1/2}. \quad (11)$$

Expression (7), [1] with R evaluated from (6) and [2] with a constant $R = 5.8 \text{ \AA}$, is shown by the solid lines in Fig. 2 in the temperature region below 1.4°K . The calculated value of (11) with M^* given by (8) is also shown for the same radii by the solid lines in the temperature region above 1.9°K . The calculated value of m^* differs from M^* by less than 20% for these radii.

In the intermediate temperature range we cannot calculate the contribution of the normal component to the effective mass, because the quasiparticle mean free path is comparable with or greater than R .

Several other experimental observations can be explained in terms of the picture of the positive ion discussed above: (1) The measured binding energy of the positive carrier to vortex rings¹⁴ has been interpreted¹⁵ as showing $R = 6.44 \pm 0.10 \text{ \AA}$, in reasonable agreement with both the low-temperature value predicted by (6), $R = 6.7 \text{ \AA}$, and the "best-fit" value, $R = 5.8 \text{ \AA}$. (2) The positive-ion mobility in He II near T_λ is observed¹⁶ to deviate from the simple $e^{\Delta/T}$ temperature dependence seen at lower temperature. The temperature range in question is just that in which viscous hydrodynamics can be applied in the normal fluid. We show in Fig. 3 the mobility calculated by applying Stokes's law

$$\mu(0) = e / [6\pi\eta R(T)], \quad (12)$$

in this temperature range.¹⁷ R has been calculated from (6). (3) The observed mobility¹⁸ in the He I region can also be accounted for by Eqs. (6) and (12). We show in Fig. 3 experimental and calculated mobilities along the vapor pressure curve. In this temperature range the variation of P_m (and consequently R) with T is significant. (4) The observed scattering cross section for the positive carrier on He³ impurities¹⁹ is also in good agreement with this picture. The cross sections for phonons and rotons¹⁹ are larger, and presumably include contributions from the electrostrictive region around

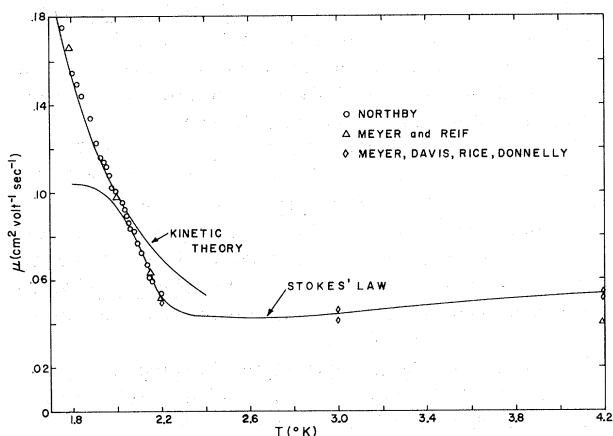


FIG. 3. Positive-ion mobility in liquid helium as a function of the temperature above 1.8°K at the vapor pressure. The curve marked kinetic theory is proportional to $e^{\Delta/T}$. The radius for the Stokes's law curve was calculated, as explained in the text, with no parameters adjusted.

the solid core.²⁰

The model which we favor for the negative carrier (the bubble model) predicts radii estimated differently by different authors. The one experimental value in the literature¹⁵ is $14.5 \pm 0.4 \text{ \AA}$. If our value of the effective mass is fitted to (8) (without a solid core contribution) the indicated value of R is $13 \pm 4 \text{ \AA}$.

We would like to acknowledge important assistance from W. Zimmerman and W. Weyhmann. We wish to thank J. A. Northby for taking mobility data between 1.8 and 2.2°K for us. We are grateful to R. L. Garwin, who first pointed out to us the possibilities of a measurement of the ac conductivity.

*This work was supported in part by the U. S. Air Force Office of Scientific Research, the U. S. Atomic Energy Commission Research Corporation, and the Alfred P. Sloan Foundation.

†Present address: Department of Physics, University of Pennsylvania, Philadelphia, Pennsylvania.

¹Preliminary accounts of this work have been given by Arnold J. Dahm and T. M. Sanders, Jr., *Bull. Am. Phys. Soc.* **10**, 1088 (1965); **11**, 362 (1966).

²K. R. Atkins, *Phys. Rev.* **116**, 1339 (1959).

³H. T. Davis, S. A. Rice, and L. Meyer, *Phys. Rev. Letters* **9**, 81 (1962).

⁴C. G. Kuper, *Phys. Rev.* **122**, 1007 (1961).

⁵A. V. Phelps, O. T. Fundingsland, and S. C. Brown, *Phys. Rev.* **84**, 559 (1951).

⁶T. S. Benedict and W. Shockley, *Phys. Rev.* **89**, 1152 (1953).

⁷C. Kittel, Introduction to Solid State Physics (John Wiley & Sons, Inc., New York, 1953), p. 235.

⁸A detailed description of the spectrometer is given in A. J. Dahm, thesis, University of Minnesota, Minneapolis, Minnesota, 1965 (unpublished).

⁹G. Feher, Bell System Tech. J. **36**, 449 (1957).

¹⁰Values for the dc mobilities were taken from F. Reif and L. Meyer, Phys. Rev. **119**, 1164 (1960).

¹¹This current reduction is apparently due to turbulence in the liquid helium near the radioactive source.

¹²L. D. Landau and E. M. Lifschitz, Fluid Mechanics (Addison-Wesley Publishing Company, Inc., Reading, Massachusetts, 1959), p. 36.

¹³G. G. Stokes, Mathematical and Physical Papers (Cambridge University Press, London, 1922), Vol. 3, p. 34; Landau and Lifschitz, op. cit., p. 96.

¹⁴A. G. Cade, Phys. Rev. Letters **15**, 238 (1965).

¹⁵P. E. Parks and R. J. Donnelly, Phys. Rev. Letters **16**, 45 (1966).

¹⁶F. Reif and L. Meyer, op. cit.

¹⁷In calculating Stokes's mobilities, viscosity data in the He II region were taken from J. T. Tough, W. D. McCormick, and J. G. Dash, Phys. Rev. **132**, 2373 (1963), and in the He I region from R. D. Taylor and J. G. Dash, Phys. Rev. **106**, 398 (1957).

¹⁸L. Meyer, H. T. Davis, S. A. Rice, and R. J. Donnelly, Phys. Rev. **126**, 1927 (1962).

¹⁹L. Meyer and F. Reif, Phys. Rev. Letters **5**, 1 (1960).

²⁰J. deBoer and A. 't Hooft, in Proceedings of the Seventh International Conference on Low-Temperature Physics, Toronto, 1960, edited by G. M. Graham and A. C. Hollis Hallett (University of Toronto Press, Toronto, Canada, 1961).

DIVERGENCE IN THE DENSITY EXPANSION OF QUANTUM-MECHANICAL TRANSPORT COEFFICIENTS

Jerome Weinstock

Institute for Telecommunication Sciences and Aeronomy, Environmental Science Services Administration,
Boulder, Colorado

(Received 8 June 1966)

It is demonstrated that the third-order term in the density expansion of quantum-mechanical transport coefficients diverges. This implies a nonanalytic density dependence for quantum gases which is in addition to the familiar nonanalytic behavior associated with quantum degeneracy. This divergence for quantum systems is completely analogous to that which was recently discovered for classical systems.

Recently, it has been independently demonstrated by several authors¹⁻⁵ that the coefficients of the third- and higher-order terms in the formal density expansion of transport coefficients diverge—for classical gases. This density-divergence situation had been previously noted for the Markoffian limit of the master equation.⁶ The tentative conclusion that has been drawn from this unexpected development is that classical transport coefficients are not analytic functions of the density. This conclusion is not unanimous, however, and there is some question⁷ about the term which is shown to be divergent in Ref. 5. As of now, the analyticity of the density dependence of classical transport coefficients remains the subject of considerable investigation, conjecture, and dispute.

The purpose of the present note is to point out that the third-order term in the density expansion of quantum-mechanical transport coefficients also diverges. This would imply a nonanalytic density dependence of quantum gases which is in addition to the familiar nonana-

lytic behavior associated with quantum degeneracy. Our method is to determine the asymptotic time dependence of a leading term in the binary-collision expansion⁸ (*t*-matrix expansion) of the third-order density coefficient. This calculation is brought into analogy with the classical case by expressing the position between particles as expectation values of Heisenberg position operators in momentum representation.

The third term in the formal density expansion of quantum transport coefficients can be given in terms of the expectation value of the four-particle collision operator $\beta_3(t)$,⁸

$$\left\langle \vec{k} \left| \frac{\partial \beta_3(t)}{\partial t} \right| \vec{k} \right\rangle \\ \equiv \int d\vec{R}_{12} d\vec{R}_{13} d\vec{R}_{14} e^{i\vec{k} \cdot \vec{R}} \frac{\partial \beta_3(t)}{\partial t} e^{-i\vec{k} \cdot \vec{R}}, \quad (1)$$

where $\beta_3(t)$ is defined in Ref. 8, \vec{R}_i denotes the position of particle *i*,

$$\vec{R}_{ij} \equiv \vec{R}_i - \vec{R}_j, \quad \vec{k} \cdot \vec{R} \equiv \sum_{i=1}^4 \vec{k}_i \cdot \vec{R}_i,$$